Short- and Long-term Mechanical Performances of Damaged Porous Asphalt Mixture Treated with Asphalt Emulsion

Abstract: Porous asphalt (PA) wearing course usually has a short service life due to the ravelling distress. Previous studies showed that spraying surface treatment (ST) asphalt emulsion could be a potential preventive maintenance technology to alleviate this distress. However, the effects of ST emulsion on the short- and long-term mechanical performances of PA mixture are still unclear, limiting the broad application of this preventive maintenance technique in practice. Therefore, this study aims to investigate the short- and long-term effects of ST emulsion on damaged PA. The repeated axial load test, indirect tensile fatigue test and indirect tensile cracking test were conducted at different curing durations to evaluate the rutting, fatigue and cracking resistances of the damaged PA specimens, respectively. Two curing temperatures, 25 ºC and 60 ºC, were considered in this study. The testing results showed that the mechanical properties of the damaged PA mixture treated with the ST emulsion were significantly improved in the short-term. The durability of mechanical properties is good based on long-term observation data. The rutting resistance of the treated PA specimen was not compromised if the application of ST emulsion is well controlled. A high curing temperature could expedite the recovery efficiency of the mechanical properties of the damaged PA, but it was accompanied by faster aging, which cannot be ignored.

Keywords: porous asphalt (PA), surface treatment (ST) emulsion, mechanical performance, durability

1 Introduction

Porous asphalt (PA) pavement is an open-graded asphalt pavement with a large air void content, which has excellent performances in reducing the tyre/road noise, alleviating the urban heat island effect and improving water permeability (Lu, Liu, et al., 2019; Lu, Renken, et al., 2019). However, compared with gap-graded or dense-graded asphalt pavements, PA usually exhibits a shorter service life. This is primarily attributed to the easy diffusion of oxygen into the pavement, which accelerates asphalt binder aging upon contact with the mortar inside PA (Li et al., 2022). Then, the cohesive and adhesive strengths gradually decline, rendering the pavement more susceptible to dislodgement of aggregates in the PA wearing course. Consequently, ravelling has become the main distress for PA pavements at the early stage. Recent studies showed that before the occurrence of the ravelling problem, timely spraying surface treatment (ST) asphalt emulsions to PA pavement could alleviate this distress and prolong the road service life (B. Xu et al., 2016; Zhang & Leng, 2017). Notably, the Netherlands Ministry of Infrastructure and Environment initiated a preventive maintenance research project on PA wearing course under the banner "Prolonging the service life of porous asphalt pavement" in 2010 (Van de Ven et al., 2013; Zhang et al., 2012). The primary goal of this project was to explore the feasibility of preventive maintenance for PA pavement through the application of ST emulsion. ST emulsions were expected to penetrate the pores of aged asphalt mixtures without clogging them and compromising the functional performances of PA pavements (Song et al., 2021). Although the ravelling problem could be alleviated by spraying this preventive maintenance material, the effects of ST emulsions on other mechanical properties of PA mixtures are rarely investigated, which is also important for the durability of PA pavement.

The fog seal applications to asphalt pavement are similar to the ST emulsion for PA pavement in terms of preventive maintenance material and usage method, which are hoped to provide some reference experience (Islam et al., 2017; L. Xu et al., 2022). Both of them are expected to repair micro-cracks of asphalt pavements and rejuvenate/soften aged asphalt binders. Estakhri and Agarwal (1991) found that a significant reduction of approximately 20% in tensile strength and a 50% increase in strain at failure were observed in the indirect tensile tests for specimens treated with fog seal. This suggested that fog seal material could significantly decrease the stiffness of the asphalt pavement, thereby improving the cracking resistance of mixture. However, there might be a concern that the permanent deformation in hot weather might increase, while there is no further field data to verify it. The main goal of fog seal technology is to seal the surface of conventional pavement, thus preventing moisture and oxygen from penetrating and diffusing into old asphalt pavements (Hu et al., 2020). In contrast, sprayed ST asphalt emulsion was expected not only to replenish the new asphalt binders to the surface and interior of the aged pavements, but also to penetrate along the voids and fill some micro-cracks in aged mortar (Jiang et al., 2022; B. Yang et al., 2022). The differences of working mechanisms between fog seal material and ST emulsion may result in different effectiveness in recovering the mechanical and functional performances of asphalt pavements, which needs further studies. Some researchers utilized the field-cored PA specimens to conduct the three-point bending beam tests before and after ST emulsion treatment. They found an increase in bending stiffness after spraying ST emulsion, while bending strength did not exhibit significant changes (Zhang, 2015). Later on, these researchers also conducted the indirect tensile test on laboratory-prepared PA specimens before and after immersion in ST emulsion containing rejuvenating components, but they didn’t observed decreasing trends in stiffness moduli and facture strengths (Zhang et al., 2016). One potential reason is the selected type of rejuvenator does not have a good compatibility with the aged binders or its dosage is too low to soften the aged asphalt binder. In addition, B. Xu et al. (2018) conducted the low-temperature cracking tests at -10 ºC to evaluate the effects of four preventive maintenance materials on PA specimens. They found that both the flexural modulus and flexural strain energy of the ST treated specimens increased, indicating the low-temperature cracking resistance of the aged PA specimens was improved.

However, apart from some limited indoor test results and successful field trials, the short- and long-term effects of ST emulsions on the mechanical performances of PA mixtures haven’t been comprehensively evaluated yet. The temporal variation law of mechanical strength of treated PA mixture remains inadequately investigated. To fill up these gaps, this study aims to investigate the rutting, fatigue and cracking resistances of ST emulsion treated PA specimens under different curing conditions. Damaged specimens were first prepared through long-term aging, followed by multiple cycles of freezing-thawing (F-T) conditioning. Then, three kinds of mechanical tests were conducted to evaluate the rutting, fatigue and cracking resistances of the treated PA specimens. Furthermore, two curing temperatures and several curing durations were considered in this study for comparison purposes. The findings of this research are expected to enhance understanding of the recovery efficiency of ST emulsion on damaged PA mixtures and promote its application in preventive maintenance strategies for porous asphalt pavements.

2 Materials and Methodology

2.1 Laboratory testing program

A typically used PA mixture with a nominal maximum aggregate size (NMAS) of 13.2 mm, denoted as PA-13, was selected in this study. A styrene-butadiene-styrene (SBS) polymer-modified asphalt binder satisfying the Superpave performance grade of 76-16 (PG76-16) and an aggregate type of granite were used. All PA specimens were compacted by the Superpave Gyratory Compactor (SGC) with a target air void content of 23% (±0.5%). The optimum asphalt content was 4.1% by weight of aggregates. Calcium hydroxide was used to improve the anti-stripping property of the PA mixture. The gradation of the PA mixture is shown in Table 1. A commonly used virgin asphalt binder in Hong Kong was selected to prepare the asphalt emulsion as the ST emulsion. A commercial cationic slow setting emulsifier was used in this study. Table 2 shows some basic properties of the ST emulsion.

Table 1. Mixture gradation of PA-13

Retained on sieve size (mm)	Weight percentage (%)	Passing percentage (%)	Lower and upper limitations (%)
16	-	100	-
13.2	7.4	92.6	90-100
9.5	25.6	67.0	40-71
4.75	52.5	14.5	10-30

2.36	2.8	11.7	9-20
1.18	3.1	8.6	7-17
0.6	2.1	6.5	6-14
0.3	1.4	5.1	5-12
0.15	0.9	4.2	4-9
0.075	1.0	3.2	3-6
Filler	1.7	-	-
Calcium hydroxide	1.5	-	-
Total aggregate	100	-	-
Asphalt content	4.1		

Table 2. Conventional properties of ST emulsion

Items	Storage stability		Evaporated residue			
	1 d	5 d	Residue content	Penetration	Softening point	Ductility
	%	%	%	25 ºC, 0.1 mm	ºC	5 ºC, cm
ST emulsion	0.3	2.1	60	64	50	67.2

To investigate the treatment effects of ST emulsions, all PA specimens were subjected to freezing-thawing (F-T) and aging conditioning to prepare damaged PA mixtures. The loose mixture was first subjected to a long-term oven aging process at 135 ºC for 8 hours (Bahia et al., 2018; Chen et al., 2021). Then, the aged loose mixtures were compacted into cylindrical specimens using the Superpave Gyratory Compactor (SGC) equipment. After that, the aged specimens were subjected to three F-T cycles in accordance with ASTM D7064 to create some micro-damages into mixtures. Finally, the ST emulsion was applied to the surface of the damaged specimen with an application rate of 0.6 kg/m^2. The treated specimens were cured at corresponding temperatures and then waited for tests. The whole conditioning process for PA specimen preparation is depicted in Figure 1. More detailed descriptions of the application conditions can be found in previous works (Jiang et al., 2022; B. Yang et al., 2022).

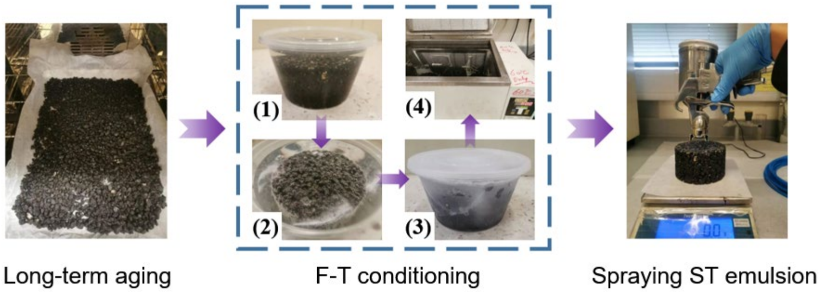

Figure 1. Conditioning processes for a PA specimen

2.2 Test methods

2.2.1 Indirect tensile asphalt cracking test

Due to the merits of being simple, practical and efficient, the indirect tensile asphalt cracking test is a popular method to characterize crack propagation in asphalt mixture (Chen et al., 2021; Yan et al., 2020; Zhou et al., 2017). In Texas, the cracking tolerance index (CT_{index}) was proposed to evaluate the cracking resistance of the asphalt mixture, which is calculated from the fracture energy (G_f), specimen dimensions, post-peak slope ($|m_{75}|$) and displacement at 75% of the peak load after the peak (l_{75}). According to the ASTM D6931 standards, the IDEAL-CT tests were conducted at 25 °C with a constant load-line displacement rate of 5 cm/min using a closed-up, feedback-controlled servo-hydraulic loading machine. Figure 2 shows the schematic of the IDEAL-CT test. The cracking tolerance index is calculated using Equations (1) - (3). $|m_{75}|$ is usually related to crack propagation and a higher value means a faster cracking rate. G_f represents the needed energy to make a specimen broken. The peak load represents the maximum value of loading force during the entire test process of a specimen.

$$G_f = \frac{W_f}{D \times t} \cdot 10^6 \tag{1}$$

$$|m_{75}| = |\frac{P_{85}-P_{65}}{l_{85}-l_{65}}| \tag{2}$$

$$CT_{index} = \frac{t}{62}\frac{l_{75}}{D}\frac{G_f}{|m_{75}|}10^6 \tag{3}$$

where CT_{index} is the cracking tolerance index; G_f is the fracture energy (J/m^2) calculated as the work of failure (the area under the load versus the average load-line displacement curve) divided by the cross-sectional area of the specimen (the product of the specimen thickness and diameter); $|m_{75}|$ is the slope of the tangential zone around the 75% peak load point after the peak; and t and D are the thickness of 62 mm and the diameter of 150 mm for the test specimen, respectively.

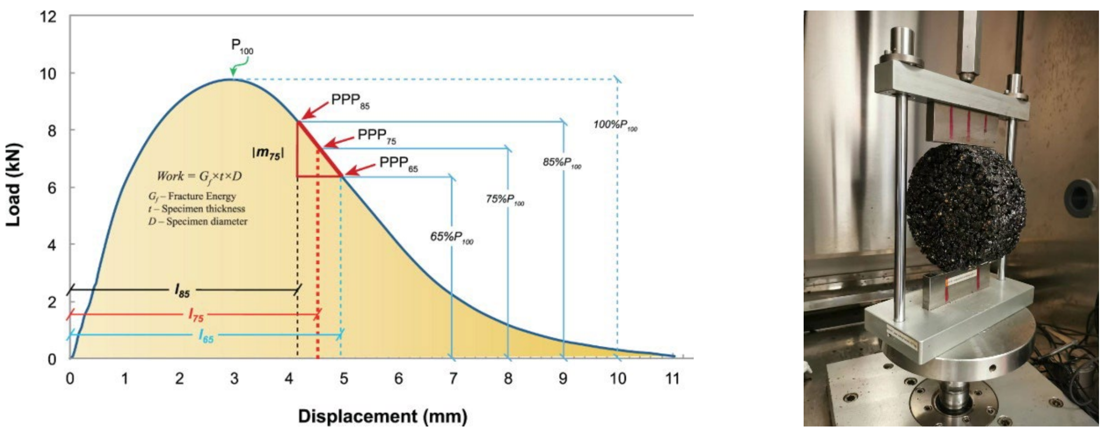

(a) (b)

Figure 2. Schematics of the IDEAL-CT test: (a) typical load-displacement curve of IDEAL-CT test (Zhou et al., 2017); and (b) set-up of IDEAL-CT test.

2.2.2 Indirect tensile fatigue test

The indirect tensile fatigue test (ITFT) was conducted at 20 °C to evaluate the fatigue resistance of the PA mixture as shown in Figure 3(a). The stress-controlled mode was selected to repeatedly apply a haversine load with 0.1 s loading time and 0.4 s rest time, which means the loading frequency is 2 Hz. The initial tensile strain should range from

70 με to 400 με during the first 10 applications in accordance with EN 12697-24. Three loading stress levels were determined after the load adjustment, which were 220, 320 and 420 kPa for lab-compacted specimens, respectively. Cylindrical specimens with a diameter of 100 mm and a thickness of 60 mm were prepared for the ITFT test. The fatigue life was obtained from the relationship curve between the decimal logarithm of the number of load cycles and the energy ratio by finding the peak energy ratio point as shown in Figure 3(b). The energy ratio can be calculated using Equation (4).

$$w_n = \frac{n}{\varepsilon_{R,n}} \cdot 10^6 \tag{4}$$

where w_n is the energy ratio at the load cycle of n; n is the number of load cycles; and $\varepsilon_{R,n}$ is the resilient strain at the load cycle number of n.

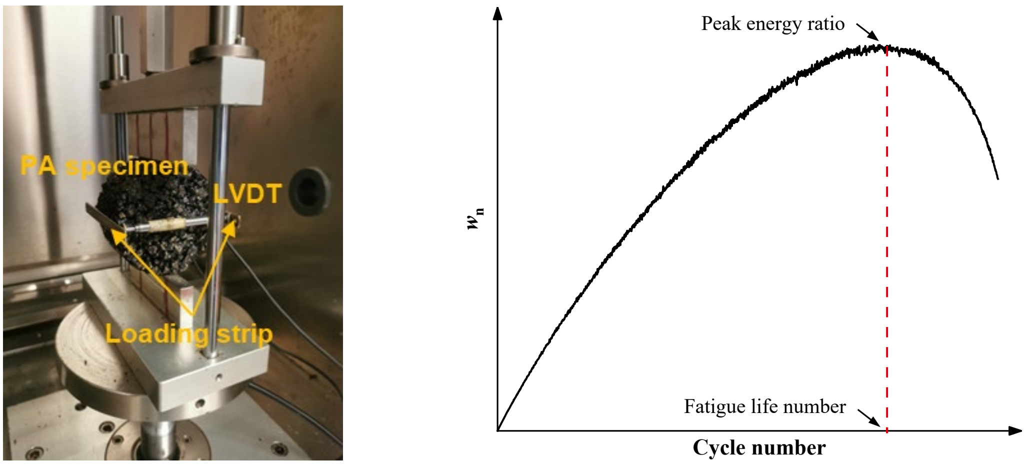

(a) (b)

Figure 3. Schematics of the ITFT test: (a) set-up of ITFT test; and (b) determination of the fatigue life based on energy concept.

2.2.3 Repeated axial load test

When ST emulsions were applied to the surface of old PA pavement, fresh ST asphalt residues will be added to existing aged pavements. It could lead to a potential threat of rutting distress, which cannot be overlooked in practice. The repeated axial load test (RALT) was selected to evaluate the rutting resistance of the asphalt mixture. A rectangular and periodical vertical stress pulse is applied to the specimen with a loading duration of 1 s and a rest period of 1 s. The loading stress, frequency and loading cycles are 100 kPa, 0.5 Hz and 3600 pulses, respectively. To observe the rutting behavior of the PA specimen in the worst case, the maximum threshold value of the test temperature specified in EN 12697-25 was selected, which is 50 ºC. Cylindrical specimens with a diameter of 150 mm and a thickness of 60 mm were prepared for this test. Figure 4 presents the schematic of the RALT test. The creep rate can be obtained from the slope of the curve at the steady creep stage. The cumulative axial strain and creep modulus can be calculated by the following Equations (5) - (7).

$$\varepsilon_n = 100 \cdot \frac{u_n}{t} \tag{5}$$

$$f_c = \frac{\varepsilon_{n1} - \varepsilon_{n2}}{n_1 - n_2} \cdot 10^4 \tag{6}$$

$$E_n = \frac{\sigma}{10 \cdot \varepsilon_n} \tag{7}$$

where ε_n is the final cumulative axial strain of specimen; f_c is the creep rate (με per loading cycle); E_n is the creep modulus (MPa); u_n is the permanent deformation of the specimen (mm); n_1 and n_2 are the numbers of repetitive loading pulses; and σ is the loading stress which is 100 kPa.

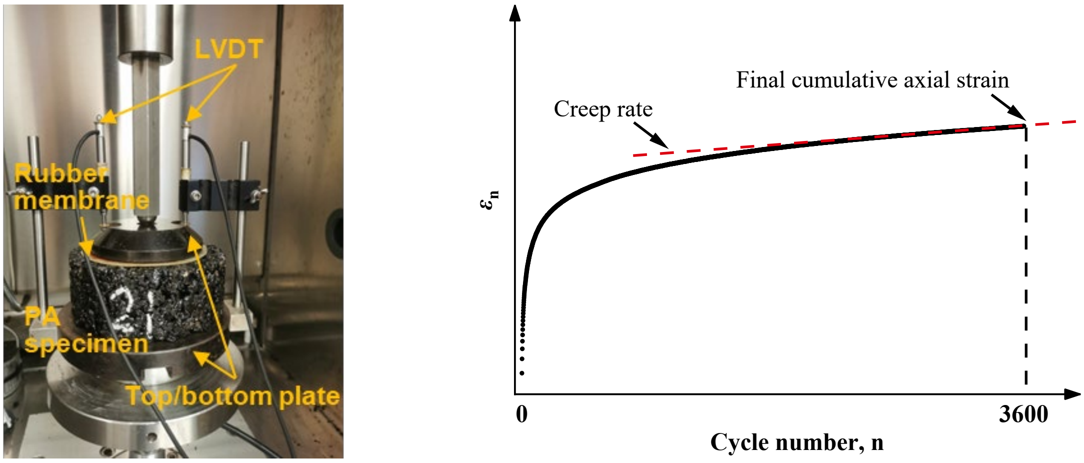

(a) (b)

Figure 4. Schematics of the RALT test: (a) set-up of RALT test; and (b) typical loading cycle number - cumulative axial strain of RALT test.

In this study, four curing durations (3, 14, 30, and 90 days) were selected to investigate the short-term and long-term mechanical performances of the specimens treated with ST emulsions. Besides, the maintenance effect could be affected by the pavement surface temperature, which is related to local weathering condition. Hong Kong has a hot summer and mild winter, which is a typical subtropical climate (J. Yang et al., 2020). So the curing temperatures of 25 °C and 60 °C were selected as a normal temperature and a higher temperature for the road surface, respectively. All aforementioned tests were conducted with at least four replicates for each test condition and a total of 124 specimens were prepared.

3 Results and Discussions

3.1 Cracking resistance of PA mixture

Figure 5 depicts the load-displacement curves of the new PA specimen, aged and F-T conditioned specimen as well as ST treated specimen. Four replicates were prepared for each scenario, and the average values of the IDEAL-CT test results were summarized in Table 3. After the long-term aging and F-T conditioning process, the vertical peak load of the damaged specimen was significantly higher than that of the unconditioned specimen. It should be noted that the long-term aging usually results in stiffer asphalt binders so that the fracture load was significantly increased. Although the aged PA specimen was then subjected to F-T conditioning, the reduction of fracture load is limited compared with the long-term aging effect. Therefore, the peak load of the damaged PA specimen was higher than that of the non-processed specimen. The decreasing trend of CT_{index} also indicates a worse cracking resistance of the damaged specimen. Meanwhile, the damaged specimen showed a higher value of $|m_{75}|$, indicating a faster deterioration rate of the post-peak load. Accordingly, the fracture energy of Gf obviously decreased for the damaged specimen. This is because the asphalt became stiffer and more brittle after aging and some micro-cracks occurred inside mortars after the F-T cycle conditioning.

Besides, compared with aging and F-T conditioned specimens, it is interesting to observe that both the peak loads of ST treated specimens cured at two temperatures gradually increased within 14 days. The possible reason is that the ST emulsion residue could replenish some fresh asphalt binders and fill some micro-cracks inside mixtures. Subsequently, the cohesive strength of aged mortar and adhesive strength between aggregates and asphalt could be improved. Later on, when specimens were cured for 90 days, The peak load of the specimen cured at 60 ºC significantly increased to 8343.67 N, while the specimen cured at 25 ºC showed a slightly higher peak load than specimens cured for 3 and 14 days. The disparity observed between the test specimens cured at two curing temperatures could be attributed to two reasons. One explanation is the diffusion efficiency between emulsion residue and old asphalt binder is higher at 60 ºC than that at the room temperature. This enhanced diffusion aids in rejuvenating the aged asphalt binder and recovering its bonding strength (B. Yang et al., 2024). On the other hand, a relatively higher curing temperature might accelerate the oxidation of asphalt binder during the long-term curing period, which also increases the peak load.

It should be noted that four indicators, CT_{index}, peak load, $|m_{75}|$ and G_f, were calculated from the loading curve, which were expected to evaluate the cracking resistance from different perspectives. It’s reasonable that all peak load results of ST treated specimens higher than damaged PA specimens, indicating the ST emulsion can help damaged PA specimen withstand a heavier traffic load. However, except for the peak load, the $|m_{75}|$ and G_f didn’t show significant improvements between ST treated and untreated PA specimens. Particularly, the CT_{index} values of ST treated specimens even exhibited worse cracking performance than untreated specimens, which is contradictory to the findings based on the peak load results. So, it's necessary to conduct more replicates and explore other types of cracking tests to comprehensively evaluate the cracking resistance of ST-treated specimens. So far, in terms of the indicator of peak load, the treated PA specimen generally showed a better cracking resistance than the untreated one.

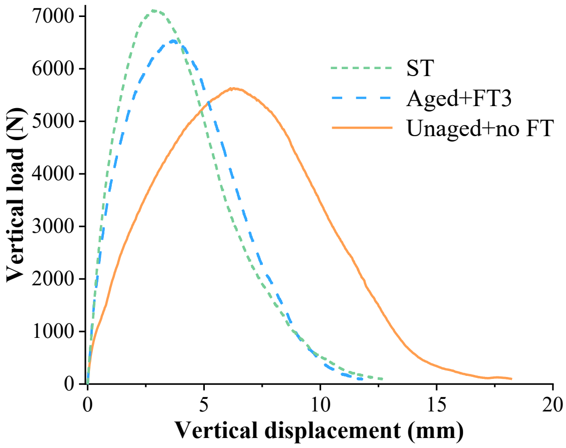

Figure 5. Load-displacement curves of IDEAL-CT

Table 3. Results of IDEAL-CT

Item	CT_{index}	Peak load N	$\lvert m_{75} \rvert$ N/m	G_f J/m^2
unaged+no FT	371.11	5911.79	871035.79	5814.49
aged+FT3	120.95	6388.90	1301823.81	4277.25
25 °C-3d-ST	105.30	6823.95	1339479.94	4445.45
25 °C-14d-ST	117.54	6603.13	1269357.05	4197.15
25 °C-90d-ST	86.94	6985.65	1456925.05	4211.32
60 °C-3d-ST	104.05	7067.94	1412321.41	4412.44
60 °C-14d-ST	109.90	6720.70	1297424.58	4461.94
60 °C-90d-ST	56.57	8343.67	1939906.03	4256.10

3.2 Fatigue resistance of PA mixture

The fatigue tests were conducted to investigate the short- and long-term effects of ST emulsion on the fatigue resistance of damaged PA specimens. The load cycle number at the maximum energy ratio was collected to estimate the fatigue life of the test specimen. Figure 6 shows the ITFT results of ST treated PA mixtures after the short-term curing. The fatigue lives of damaged specimens at the stress levels of 220 kPa, 320 kPa and 420 kPa are 17636, 3899 and 1121 cycles, respectively. Compared with the damaged specimen, which was subjected to aging and F-T conditioning only, the ST treated specimen obviously presented a better fatigue resistance. When the curing temperature is 25 °C, the fatigue lives of the treated specimens at the stress levels of

220 kPa, 320 kPa and 420 kPa increased to 19642, 4446 and 1730 cycles, respectively. This is because after the ST emulsions were sprayed to the surface of a specimen, emulsions penetrated damaged specimens, replenishing fresh asphalt binders and filling up some micro-cracks inside mixtures. In addition, when the curing temperature is 60 ºC, the fatigue lives corresponding to the low/medium/high stress (220/320/420 kPa) for ST treated specimens were 28,686, 4,921 and 1,855 cycles, respectively, which were 63%, 26% and 65% higher than those of the damaged specimens without emulsion treatment. This indicates that a high curing temperature can improve the recovery efficiency of fatigue resistance in the short term.

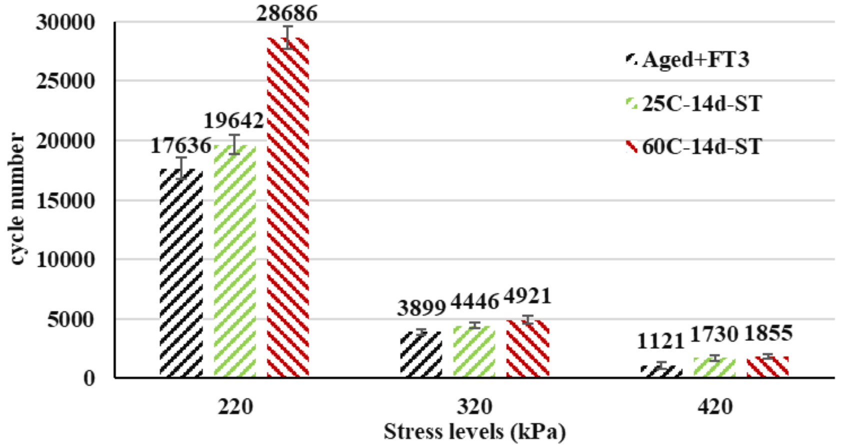

Figure 6. Fatigue lives of PA specimens after a short-term curing period

The fatigue lives of different specimens after 90 days of curing are shown in Figure 7. Even after a long-term curing, specimens treated with ST emulsion still kept a better fatigue resistance than untreated specimens, indicating that the recovery efficiency of ST emulsion on fatigue resistance has good durability. In addition, compared with Figure 6, specimens cured for 90 days showed higher fatigue lives than specimens cured for 14 days as shown in Figure 7. One possible explanation is that long-term curing leads to the aging of asphalt, which increases the resilient modulus of a PA specimen (Liang & Lee, 1996). Thus, when the same stress level was applied to specimens, specimens after 90 days of curing displayed a lower initial resilient strain as shown in Table 4, which means that specimens have a better ability to bear the current loading condition. So, compared with the short-term cured specimen, the long-term cured specimen showed a longer fatigue life under the controlled-stress loading mode.

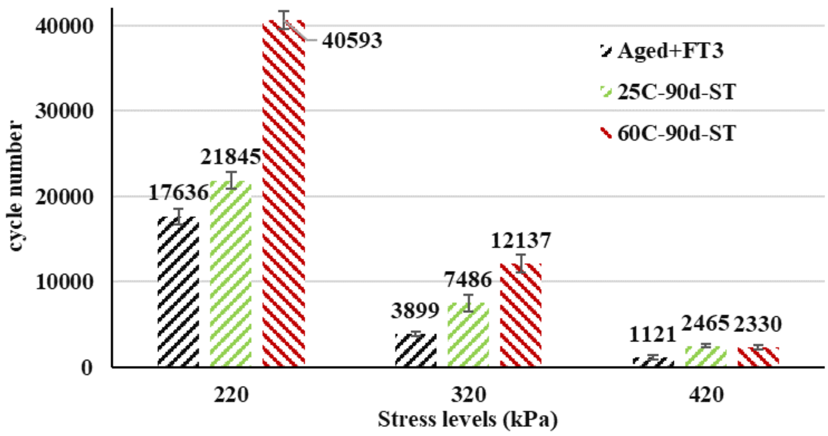

Figure 7. Fatigue lives of PA specimens after a long-term curing period

Table 4. Initial tensile strains of PA specimens after a long-term curing period

Item	Initial tensile strain at different stresses (με)		
	220 kPa	320 kPa	420 kPa
Aged + FT3	117.3	183.9	277.0
25 °C-14d-ST	106.5	165.8	229.6
25 °C-90d-ST	105.6	161.0	223.8
60 °C-14d-ST	98.8	164.5	213.1
60 °C-90d-ST	89.0	140.8	200.4

3.3 Rutting resistance of PA mixture

From the RALT test, the following three performance parameters of the PA specimens are commonly obtained: cumulative axial strain (ε_n), creep rate (f_c) and creep modulus (E_n). Figure 8 shows the RALT test results of ST treated specimens at two different curing temperatures within three months. The ε_n and f_c of ST treated specimens were obviously lower than those of untreated PA specimens, indicating a good rutting resistance performance of the treated specimens. It was unexpected because spraying ST emulsion on asphalt pavement can increase the asphalt content of mixture, which tends to generate the rutting distress of the top layer as mentioned in other studies (Estakhri & Agarwal, 1991; Raad et al., 2001). A possible explanation is that asphalt emulsion was usually applied to the dense-graded pavement as a preventive maintenance technology, like the fog seal, while the ST emulsion used in this study was applied to the PA pavement and the emulsion will penetrate inside mixture without clogging the voids or accumulating on the pavement surface. Thus, the potential rutting problem may not be aggravated as long as the application rate and the viscosity of ST emulsion are well controlled. A similar phenomenon was also observed in another study (Qureshi et al., 2013).

In addition, the treated specimens cured at 60 °C showed higher ε_n values than those cured at room temperature during the whole curing period, which means a deeper cumulative permanent deformation. One possible reason is that the newly added ST residue might diffuse with aged mortar and a higher curing temperature could accelerate the diffusion rate. This can also be explained by the variation trend of indicator E_n. During the short-term curing period, after 14 days of curing, both treated specimens cured at two temperatures showed a high creep modulus than untreated specimens, indicating that spraying ST emulsion to a damaged PA specimen can improve cohesive and adhesive strengths by filling up micro-cracks and thickening the mortar films. Interestingly, the E_n of treated specimens cured at 60 °C is 6.91 MPa, while that at 25 °C is 9.69 MPa, which implies a high curing temperature can improve the diffusion efficiency of the new ST residue in the aged asphalt mortar, then further softens the aged asphalt binders. However, during the long-term curing period, the treated specimens were more sensitive to the aging phenomenon due to the high curing temperature of 60 °C, so the E_n of treated specimens gradually increased to 7.65 MPa after 90 days of curing. By contrast, the treated specimens were less sensitive to the aging problem at room temperature and the diffusion phenomenon might keep on going at the same time, so the E_n of treated specimens gradually decreased to 8.18 MPa after 90 days of curing. Overall, the rutting resistance of the damaged PA specimen could be improved after the ST emulsion was applied.

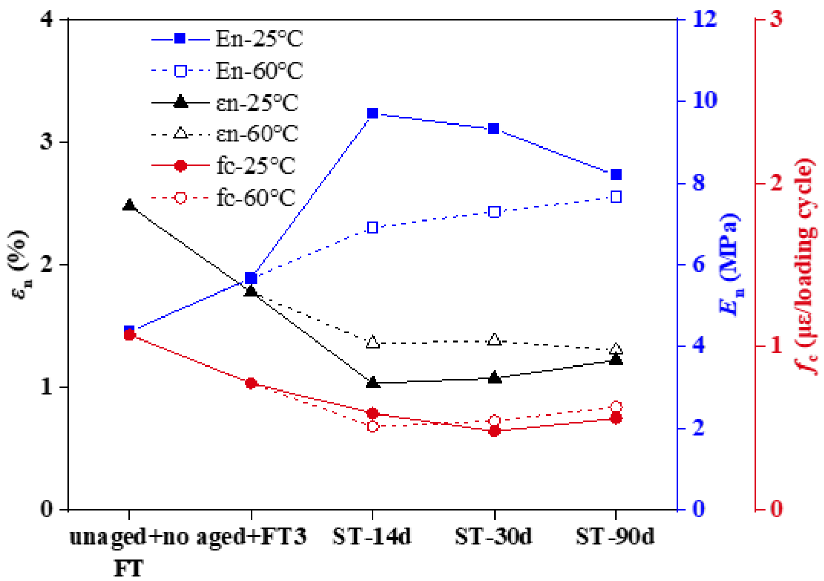

Figure 8. RALT test results of PA specimens

3.4 Statistical analysis

To statistically evaluate the effects of ST emulsion on the mechanical properties of damaged PA specimens, significant difference analyses were conducted 1) between specimens treated with and without ST emulsions, 2) between different curing temperatures. Table 5, 6 and 7 summarize the statistical results of cracking, fatigue and rutting properties for different PA specimens, respectively. Codes N, S and HS represents no significant difference ($P > 0.05$), significant difference ($0.01 < P < 0.05$) and highly significant difference ($P < 0.01$), respectively.

It can be seen from Table 5 that all damaged PA specimens treated with ST emulsion had highly significant different peak load values from the damaged PA specimens that treated without any maintenance material, indicating the contribution of ST emulsion. And curing temperatures have significant different peak load values between ST treated specimens. However, different evaluating indicators may have different sensitivities to the maintenance effectiveness. Insignificant differences were found in several comparison scenarios when using indicators of CT_{index}, $|m_{75}|$ or G_f to evaluate the ST emulsion effect and curing temperature effect on cracking performance. Table 6 shows that regardless of the applied stress levels and curing periods, the fatigue properties of PA specimens treated with and without ST emulsions indicated significant differences. And fatigue resistance differences were also found at the low/medium stress levels under different curing temperatures. Finally, statistical results in Table 7 suggest that the ST emulsion could significantly improve the rutting properties of damaged PA specimens. And the curing temperature could make a difference among the rutting properties of ST treated specimens. Overall, the ST emulsion could statistically improve the cracking, fatigue and rutting resistance of damaged PA specimens. And conducting the preventive maintenance work at a hot weather could promote the recovery efficiency of mechanical properties of PA.

Table 5. Significant analysis of cracking performance of different PA specimens

Item	Cracking performance			
	CT_{index}	Peak load	$\|m_{75}\|$	G_f
ST emulsion effect				
aged+FT3 vs 25 ºC-3d-ST	S	HS	S	S
aged+FT3 vs 25 ºC-14d-ST	N	HS	S	N
aged+FT3 vs 25 ºC-90d-ST	HS	HS	S	S
aged+FT3 vs 60 ºC-3d-ST	S	HS	S	S
aged+FT3 vs 60 ºC-14d-ST	S	HS	N	S
aged+FT3 vs 60 ºC-90d-ST	HS	HS	HS	N
Curing temperature effect				
25 ºC-3d-ST vs 60 ºC-3d-ST	N	S	S	N
25 ºC-14d-ST vs 60 ºC-14d-ST	N	S	S	S
25 ºC-90d-ST vs 60 ºC-90d-ST	HS	HS	HS	N

Note: N: no significant difference ($P > 0.05$); S: significant difference ($0.01 < P < 0.05$), HS: highly significant difference ($P < 0.01$).

Table 6. Significant analysis of fatigue performance of different PA specimens

Item	Fatigue life		
	220 kPa	320 kPa	420 kPa
ST emulsion effect			
aged+FT3 vs 25 ºC-14d-ST	HS	S	S
aged+FT3 vs 25 ºC-90d-ST	HS	HS	HS
aged+FT3 vs 60 ºC-14d-ST	HS	HS	HS
aged+FT3 vs 60 ºC-90d-ST	HS	HS	HS
Curing temperature effect			
25 ºC-14d-ST vs 60 ºC-14d-ST	HS	S	N
25 ºC-90d-ST vs 60 ºC-90d-ST	HS	HS	N

Note: 220/320/420 kPa means the stress level of fatigue test.; S: significant difference ($0.01 < P < 0.05$), HS: highly significant difference ($P < 0.01$).

Table 7. Significant analysis of rutting performance of different PA specimens

Item	Rutting performance		
	ε_n	f_c	E_n
ST emulsion effect			
aged+FT3 vs 25 ºC-14d-ST	HS	S	HS
aged+FT3 vs 25 ºC-30d-ST	HS	S	HS
aged+FT3 vs 25 ºC-90d-ST	HS	S	HS
aged+FT3 vs 60 ºC-14d-ST	HS	S	HS

aged+FT3 vs 60 °C-30d-ST	HS	S	HS
aged+FT3 vs 60 °C-90d-ST	HS	S	HS
Curing temperature effect			
25 °C-14d-ST vs 60 °C-14d-ST	HS	S	HS
25 °C-30d-ST vs 60 °C-30d-ST	HS	S	HS
25 °C-90d-ST vs 60 °C-90d-ST	S	S	S

Note: S: significant difference ($0.01 < P < 0.05$), HS: highly significant difference ($P < 0.01$).

4 Findings and Conclusions

This study investigated the short- and long-term effects of ST emulsion on the mechanical performances of damaged porous asphalt mixture. The durabilities of the cracking, rutting and fatigue resistances of the treated PA mixture were systematically analyzed. Below are the main findings and conclusions summarized as follows:

- After the ST emulsion was applied to the damaged PA specimen, the treated specimen can acquire a higher indirect tensile strength, a longer fatigue life and a better anti-rutting performance than untreated PA specimen in the short-term.
- Compared with the damaged PA specimen, the ST treated PA specimen kept a good mechanical performance within 3 months, indicating a good durability of mechanical performance, which is helpful to extend the service life of PA pavement.
- Although a relatively high curing temperature can accelerate the recovery efficiency of mechanical properties of damaged PA in the short term, a relatively fast aging phenomenon also accompanies with it, which cannot be neglected. Therefore, a ST emulsion with an excellent anti-aging property is expected to achieve a better maintenance effect for PA.

- When the appropriate ST emulsion material and application conditions are well designed, the rutting resistance of the treated PA specimen is not compromised in the scenarios considered in this study.

Despite the interesting findings of this study, it is worth noting that only one type of ST emulsion was selected in this study. More ST emulsions containing different rejuvenators or modifiers should be considered in the future to compare their mechanical recovery efficiencies of PA specimens. Besides, the improvement effects of mechanical durability due to aging and curing should be clearly distinguished, and trial tests should be conducted in the field for verification.

Disclosure statement

The authors report there are no competing interests to declare.

References

Bahia, H. U., Sadek, H., Rahaman, M. Z., Lemke, Z., Swiertz, D., Reichelt, S., & Bitumix Solutions, L. (2018). *Field aging and oil modification study* (PDF). W. D. o. Transportation. https://rosap.ntl.bts.gov/view/dot/40770

Chen, H., Zhang, Y., & Bahia, H. U. (2021). The role of binders in mixture cracking resistance measured by ideal-CT test. *International journal of fatigue*, *142*, 105947. https://doi.org/10.1016/j.ijfatigue.2020.105947

Estakhri, C., & Agarwal, H. (1991). *Effectiveness of Fog Seal and Rejuvenators for Bituminous Pavement Surfaces. Final Report* (No. FHWA/TX-91/1156-1F, Res Rept 1156-1F, TTI: 2-18-87-1156

Hu, C., Li, R., Zhao, J., Leng, Z., & Lin, W. (2020). Performance of Waterborne Epoxy Emulsion Sand Fog Seal as a Preventive Pavement Maintenance Method: From Laboratory to Field. *Advances in materials science and engineering*, *2020*. https://doi.org/10.1155/2020/6425817

Islam, R. M., Arafat, S., & Wasiuddin, N. M. (2017). Quantification of reduction in hydraulic conductivity and skid resistance caused by fog seal in low-volume roads. *Transportation Research Record*, *2657*(1), 99-108.

Jiang, J., Leng, Z., Yang, B., Lu, G., Tan, Z., Han, M., & Dong, Z. (2022). Penetration mechanism of the emulsion-based rejuvenator in damaged porous asphalt mixture: Microstructure characterization and 3D reconstruction. *Materials & Design*, *221*, 111014. https://doi.org/10.1016/j.matdes.2022.111014

Li, D., Leng, Z., Wang, H., Chen, R., & Wellner, F. (2022). Structural and mechanical evolution of the multiphase asphalt rubber during aging based on micromechanical back-calculation and experimental methods. *Materials & Design*, *215*, 110421. https://doi.org/https://doi.org/10.1016/j.matdes.2022.110421

Liang, R. Y., & Lee, S. (1996). Short-term and long-term aging behavior of rubber modified asphalt paving mixture. *Transportation Research Record*, *1530*(1), 11-17.

Lu, G., Liu, P., Wang, Y., Faßbender, S., Wang, D., & Oeser, M. (2019). Development of a sustainable pervious pavement material using recycled ceramic aggregate and bio-based polyurethane binder. *Journal of Cleaner Production*, *220*, 1052-1060. https://doi.org/https://doi.org/10.1016/j.jclepro.2019.02.184

Lu, G., Renken, L., Li, T., Wang, D., Li, H., & Oeser, M. (2019). Experimental study on the polyurethane-bound pervious mixtures in the application of permeable pavements. *Construction and Building Materials*, *202*, 838-850. https://doi.org/https://doi.org/10.1016/j.conbuildmat.2019.01.051

Qureshi, N. A., Tran, N. H., Watson, D., & Jamil, S. M. (2013). Effects of rejuvenator seal and fog seal on performance of open-graded friction course pavement. *Maejo International Journal of Science and Technology*, *7*(2), 189.

Raad, L., Saboundjian, S., & Minassian, G. (2001). Field aging effects on fatigue of asphalt concrete and asphalt-rubber concrete. *Transportation Research Record*, *1767*(1), 126-134.

Song, W., Huang, B., Shu, X., Chandler, M., Woods, M., & Jia, X. (2021). Laboratory Investigation of Fog-Seal Treatment on Performance of Open-Graded Friction Course Pavement. *Journal of materials in civil engineering*, *33*(3). https://doi.org/10.1061/(ASCE)MT.1943-

5533.0003619
Van de Ven, M., Qiu, J., & Zhang, Y. (2013). Increasing the functional service life of porous surfacings: Development of test methods to study the effect of rejuvenating binders. (Ed.),^(Eds.). Proceeding of 15th International Flexible Pavements Conference of AAPA, Australian Asphalt Pavement Association, Queensland, Australia.
Xu, B., Chen, J., Li, M., Cao, D., Ping, S., Zhang, Y., & Wang, W. (2016). Experimental investigation of preventive maintenance materials of porous asphalt mixture based on high viscosity modified bitumen. *Construction & building materials*, *124*, 681-689. https://doi.org/10.1016/j.conbuildmat.2016.07.122
Xu, B., Li, M., Liu, S., Fang, J., Ding, R., & Cao, D. (2018). Performance analysis of different type preventive maintenance materials for porous asphalt based on high viscosity modified asphalt. *Construction & building materials*, *191*, 320-329. https://doi.org/10.1016/j.conbuildmat.2018.10.004
Xu, L., Jiang, C., & Xiao, F. (2022). Application of Fog-Seal Technology with Waterborne Thermosetting Additive in Asphalt Pavement. *Journal of materials in civil engineering*, *34*(8), 04022160.
Yan, C., Zhang, Y., & Bahia, H. U. (2020). Comparison between SCB-IFIT, un-notched SCB-IFIT and IDEAL-CT for measuring cracking resistance of asphalt mixtures. *Construction and Building Materials*, *252*, 119060.
Yang, B., Leng, Z., Jiang, J., Chen, R., & Lu, G. (2024). Diffusion characteristics of surface treatment emulsion in aged asphalt mortar of porous asphalt mixture through SEM/EDS analysis. *International Journal of Pavement Engineering*, *25*(1), 2290093.
Yang, B., Leng, Z., Jiang, J., He, Z., & Li, D. (2022). Recovery efficiency of the damaged porous asphalt mixture with emulsion-based surface treatment: Material optimization and performance verification. *Construction and Building Materials*, *347*, 128530. https://doi.org/https://doi.org/10.1016/j.conbuildmat.2022.128530
Yang, J., Wong, M. S., Ho, H. C., Krayenhoff, E. S., Chan, P. W., Abbas, S., & Menenti, M. (2020). A semi-empirical method for estimating complete surface temperature from radiometric surface temperature, a study in Hong Kong city. *Remote sensing of environment*, *237*, 111540. https://doi.org/https://doi.org/10.1016/j.rse.2019.111540
Zhang, Y. (2015). *Extending the Lifespan of Porous Asphalt Concrete*, Delft University of Technology]. http://resolver.tudelft.nl/uuid:f9860e45-e28b-477b-8df9-a094b00fd703
Zhang, Y., & Leng, Z. (2017). Quantification of bituminous mortar ageing and its application in ravelling evaluation of porous asphalt wearing courses. *Materials & Design*, *119*, 1-11. https://doi.org/https://doi.org/10.1016/j.matdes.2017.01.052
Zhang, Y., van de Ven, M. F. C., Molenaar, A. A. A., & Wu, S. P. (2016). Assessment of effectiveness of rejuvenator on artificially aged porous asphalt concrete. *Construction and Building Materials*, *110*, 286-292. https://doi.org/https://doi.org/10.1016/j.conbuildmat.2016.02.042
Zhang, Y., Ven, M. F. C. v. d., Molenaar, A. A. A., & Wu, S. (2012). Increasing the Service Life of Porous Asphalt with Rejuvenators (*Sustainable Construction Materials 2012* (pp. 318-330). https://doi.org/https://doi.org/doi:10.1061/9780784412671.0027
Zhou, F., Im, S., Sun, L., & Scullion, T. (2017). Development of an IDEAL cracking test for asphalt mix design and QC/QA. *Road Materials and Pavement Design*, *18*(sup4), 405-427.

https://doi.org/10.1080/14680629.2017.1389082